Computational investigation of aza-18-crown-6 derivatives as iron corrosion inhibitors

Nur Asia, Eka Junaidi, Saprizal Hadisaputra*

Chemistry Education Division, University of Mataram. Jalan Majapahit No 62, Mataram, 83125, Indonesia

*Corresponding Author:
Email*: rizal@unram.ac.id

Revised: February 4, 2026
Accepted: Mei 29, 2026

DOI: 10.1980/jses.v1i1.2

Phone*: +6287738066422

Abstract: *The effect of changes in the number of nitrogen atoms on the corrosion inhibition efficiency of 1,4,7,10,16-Pentaoxa-13-azacyclooctadecane (aza-18-crown-6/N1) derivatives has been studied using Density Functional Theory and Monte Carlo Simulation. The DFT B3LYP/6-311G(d,p) method was used to measure the quantum parameters of aza-18-crown-6 derivatives. Prediction of corrosion inhibition efficiency based on quantum parameters is successively hexaaza-18-crown-6 (N6) > pentaaza-18-crown-6 (N5) > tetraaza-18-crown-6 (N4) > triaza-18-crown-6 (N3) > 1,4,10,13-diaza-18-crown-6 (N2) > aza-18-crown-6 (N1). N6 has the highest inhibition efficiency, while N1 has the lowest. The substitution of a nitrogen atom into the crown ether ring acts as an electron donor. Monte Carlo simulations demonstrate the interaction of aza-18-crown-6 derivatives with the iron surface. This indicates good agreement with the results obtained from DFT/B3LYP 6-311G (d,p) quantum calculations in the solution phase.*

Keywords: *corrosion inhibitor, aza-18-crown-6, DFT, Monte Carlo simulation*

Introduction

Corrosion causes metal surfaces to become rough, brittle, and easily destroyed. The corrosion process is quite difficult to control. Preventative measures are necessary to reduce corrosion [1, 2]. The use of corrosion inhibitors is an effective, efficient, and economical way to prevent corrosion. Corrosion inhibitors generally come from inorganic and organic compounds. Organic inhibitors are the right solution for preventing corrosion because they are readily available, safe, inexpensive, and environmentally friendly. Organic compounds used as inhibitors must contain at least one heteroatom, such as N, O, P, or S, which has a lone pair of π electrons [3, 4].

One organic compound that can be used as a corrosion inhibitor is a crown ether compound. Crown ethers have the advantage of effectively binding metal ions through complex formation. Crown ethers have structural properties that can be easily modified to meet the criteria for corrosion inhibitors, due to their heteroatoms (O, N, P, and S) in their structure. Furthermore, crown ethers are non-toxic and environmentally friendly, making them suitable for use as corrosion inhibitors [5-10].

Fouda et al. [10] reported that crown ethers have great potential as corrosion inhibitors due to their high efficiency. M. Abdallah et al. (2008) investigated 18-Crown-6-ether (DB18C6) derivatives using the mass loss method and found an efficiency of 72% on type 304 stainless steel in hydrochloric acid (HCl). Fouda et al. (2010) also studied the effect of several crown ethers as corrosion inhibitors on type 430 stainless steel in 2M hydrochloric acid (HCl) and obtained an efficiency of 82.02%. Paul et al. [11] also studied the potential of dibenzo-18-crown-6 derivatives as corrosion inhibitors on mild steel in hydrochloric acid (HCl) solution and obtained an efficiency of 98.57%.

Studies on the use of crown ethers as corrosion inhibitors have also been discussed through theoretical studies. The influence of macrocyclic ring size on corrosion inhibition efficiency of dibenzo-crown-ethers using DFT method. Furthermore, theoretical studies on the efficiency of crown ethers as corrosion inhibitors are still limited to crown ether compounds with the addition of substituents only. Therefore, theoretical research is needed on the influence of the type of heteroatom bonded to the crown ether ring (Figure 1) that can increase corrosion inhibition efficiency.

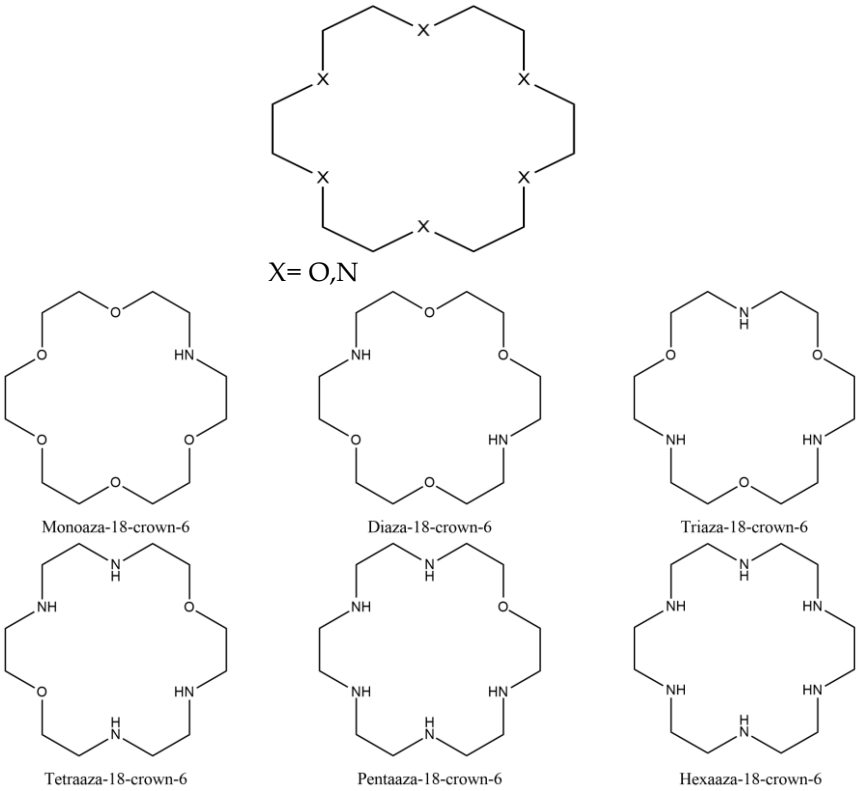

Figure 1 Structure of the Aza-18-Crown-6 derivative compound (O = Oxygen, N = Nitrogen).

Methodology

Theoretical Inhibition Data Analysis

The ionization potential can be calculated using Equation (1):

$$I = -E_{HOMO} \quad (1)$$

where I is the ionization potential and E_HOMO is the energy of the Highest Occupied Molecular Orbital [12].

The electron affinity can be calculated using Equation (2):

$$A = -E_{LUMO} \quad (2)$$

where A is the electron affinity and E_LUMO is the energy of the Lowest Unoccupied Molecular Orbital [12].

Electronegativity can be calculated using Equation (3):

$$X = (I+A)/2 \quad (3)$$

where χ is the electronegativity, I is the ionization potential, and A is the electron affinity [13].

Hardness can be calculated using Equation (4):

$$\eta = (I-A)/2 \quad (4)$$

where η is the chemical hardness, I is the ionization potential, and A is the electron affinity [14].

The fraction of electron transfer (ΔN) can be calculated using Equation (5):

$$\Delta N = \frac{X_{Fe} - X_{inh}}{2(\eta Fe + \eta inh)} \quad (5)$$

where ΔN is the electron transfer, χ_Fe is the electronegativity of iron, χ_inh is the electronegativity of the inhibitor, η_Fe is the hardness of iron, and η_inh is the hardness of the inhibitor. Based on theoretical values, χ_Fe = 7.0 eV and η_Fe = 0 are used to calculate the fraction of electron transfer [15].

The theoretical corrosion inhibition efficiency was calculated using Equations (6), (7), and (8):

$$\text{Iadd.}\% = \frac{I_{Inh} - I_{X-Inh}}{I_{Inh}} X\ 100 \quad (6)$$

$$\text{IEadd.}\% = I_{add}.\% - I_{eInh}.\% \quad (7)$$

$$IEteori.\% = I_{eInh.}\% + IE_{add}.\% \quad (8)$$

where I_add.% is the percentage of ionization potential difference, I_Inh is the ionization potential of the parent compound, I_X is the ionization potential of the derivative compound, IE_add.% is the additional inhibition efficiency percentage, IE_Inh.% is the inhibition efficiency, and IE_theory.% is the theoretical inhibition efficiency percentage.

Simulasi Monte Carlo

Monte Carlo simulations were performed using Material Studio 7.0 software from Accelrys Inc. This Monte Carlo simulation process can find the lowest energy adsorption site of organic inhibitors on metal surfaces and water molecules. The initial step taken was to save the crown ether structure optimization results from Gaussian in MDL SDfile (.sdf) format so that they can be imported into the material studio system in 3D. Next, select the iron metal surface used as the Fe (110) plane, because the Fe (110) crystal plane is the most stable for simulating the adsorption process [17]. To provide a large surface for the interaction of organic inhibitors, Supercell (8x8) and Vacuum slab with a thickness of 15 Å along the C axis were used, built with the Fe (110) plane. All simulations were implemented with the KOMPASS force field to optimize the structure of all desired system components. Organic inhibitors (monoaza-18-crown-6, diaza-18-crown-6, triaza-18-crown-6, tetraaza-18-crown-6, pentaaza-18-crown-6, hexaaza-18-crown-6) and Fe (110) using 100 molecules in each case or each organic inhibitor. The use of 100 water molecules is very important in the simulation because it can play an important role in corrosion in the environment [18].

Result and Discussion

As a consequence of selecting a quantum chemistry method, method validation is necessary. Optimization of the structure of aza-18-crown-6 derivatives was performed based on the experimental crystal structure. The optimized structure of aza-18-crown-6 derivatives, represented by hexaaza-18-crown-6 (N6), is shown in Figure 2.

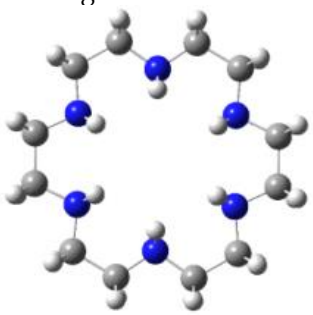

Figure 2. Structure Optimization Results of Hexaza-18-Crown-6 Compound (atoms: white=H; blue=N; gray=C)

Table 1. Comparison of structural parameters of 18-crown-6 and derivatives of aza-18-crown-6.

Senyawa	Diagonal O-O Distance					
	DFT		*Ab initio*		Experiment	
	Min (Å)	Max (Å)	Min (Å)	Max (Å)	Min (Å)	Max (Å)
18C6 (N0)	5.381	5.385	5.802	5.948	4.267	4.784
N1	5.568	5.848				
N2	5.587	5.808				
N3	5.831	5.836				
N4	5.509	5.978				
N5	5.771	5.972				
N6	5.622	5.627				

Table 1 shows the bond distance between O-O from the structure optimization results with DFT calculations for the compound 18-crown-6 (18C6) obtained the shortest bond distance of 5.381 Å and the longest bond distance of 5.385 Å. These results are not much different from the crystal structure of the experimental results conducted by Dunitz (1974) [19] who reported the shortest O-O bond distance of 4.267 Å and the longest bond distance of 4.784 Å. The difference in bond distance between the theoretical and experimental calculation data shows good results, namely an average of around ~0.6-1 Å. In the *ab initio* calculation, the results of the difference in bond distances were quite different when compared to the results of the DFT calculation, where the longest bond

distance was 5.948 Å and the shortest bond distance was 5.802 Å. Thus, based on the comparison of shorter bond distances, the use of the DFT method at the B3LYP level of theory with the 6-31G(d) basis set is more valid and acceptable for optimizing the molecular structure of aza-18-crown-6 derivative compounds.

Quantum Chemistry Parameters

Table 2 shows that the addition of nitrogen (N) heteroatoms affects the corrosion inhibition efficiency of aza-18-crown-6 derivatives. The order of corrosion inhibition efficiency, according to Table 4.2, is hexaaza-18-crown-6 (N6) > pentaaza-18-crown-6 (N5) > tetraaza-18-crown-6 (N4) > triaza-18-crown-6 (N3) > diaza-18-crown-6 (N2) > monoaza-18-crown-6 (N1). The increase in inhibition efficiency of these organic inhibitors can be explained based on adsorption theory, which assumes that organic inhibitors form a protective layer/film on the metal surface. It is known that adsorption primarily depends on the presence of π electrons and heteroatoms, which leads to greater adsorption of inhibitor molecules on the metal surface. Compounds containing nitrogen (N) and sulfur (S) are important because they often provide superior inhibition compared to compounds containing only nitrogen or sulfur [20].

Table 2. Quantum chemical parameters for aza-18-crown-6 derivatives calculated using DFT at the B3LYP/6-31G(d,p) level of theory.

Inhibitor	Parameters							
	E_{HOMO} (eV)	E_{LUMO} (eV)	Egap (eV)	*I* (eV)	*A* (eV)	*X* (eV)	ΔN (eV)	IE_{theory} (%)
N1-18C6	-6.18814	1.15947	7.34761	6.18814	-1.15947	2.51433	0.61049	60.81247
N2-18C6	-6.12963	1.06695	7.19658	6.12963	-1.06695	2.53134	0.62094	61.43564
N3-18C6	-6.05154	1.08818	7.13972	6.05154	-1.08818	2.48168	0.63284	62.26735
N4-18C6	-5.82840	0.95348	6.78188	5.82840	-0.95348	2.43746	0.67275	64.64393
N5-18C6	-5.77861	0.95648	6.73509	5.77861	-0.95648	2.41106	0.68134	65.17422
N6-18C6	-5.60364	0.28544	5.88908	5.60364	-0.28544	2.65909	0.73710	67.03776

The aza-18-crown-6 derivative compounds in their structure contain heteroatoms such as nitrogen (N) which have lone electron pairs. Each aza-18-crown-6 derivative compound that has lone electron pairs on the nitrogen atom (N) interacts with the d-orbitals of iron metal (Fe) to form a protective layer/film that can inhibit the corrosion rate and increase corrosion inhibition efficiency. Table 2 shows the highest inhibition efficiency is found in the hexaaza-18-crown-6 (N6) compound inhibitor at 67.03% while the lowest efficiency is found in the monoaza-18-crown-6 (N1) compound inhibitor at 60.81%.

The difference in inhibition efficiency of these organic inhibitors of aza-18-crown-6 derivative compounds is caused by the addition of different nitrogen (N) heteroatoms to the crown ether ring which will affect its structure and electron density. Based on studies of several organic compounds containing nitrogen (N) atoms for iron corrosion inhibition, the presence of electron density on the atoms of functional groups, which serve as reaction centers, emphasizes the effectiveness of organic compound inhibition. The inhibition efficiency of organic inhibitors increases with increasing electron density on the nitrogen (N) atom, which serves as the reaction center for aza-18-crown-6 derivatives. Thus, the addition of more nitrogen (N) heteroatoms to hexaaza-18-crown-6 (N6) compounds increases the electron density in their molecular structure, thereby facilitating stronger adsorption on iron (Fe) metal surfaces and higher inhibition efficiency than other inhibitor compounds.

The addition of nitrogen (N) heteroatoms to the crown ether ring of aza-18-crown-6 derivatives is also explained by the HSAB (Hard Soft Acid Base) theory. Based on the theory of acid-base strength (HSAB) introduced by Pearson (1968) [21], nitrogen atom donors are more basic (base strength n = 7.27) than oxygen atom donors (base strength n = 6.08). This difference, of course, serves as a reference for the study of heteroatom changes conducted in this study. According to the HSAB principle, hard acids are more stable when forming complexes with hard bases, and soft acids are

more stable when forming complexes with soft bases.

Based on HSAB, iron (Fe) as the central atom is included in the "hard" group, while ligands from aza-18-crown-6 derivatives contain nitrogen (N) heteroatoms as bases, so the bonding tendency is covalent and coordinate covalent. Coordination covalent bonds occur due to the presence of empty d orbitals on the iron metal atom (Fe) so that the electron pairs owned by the nitrogen atom (N) in the aza-18-crown-6 ligand and its derivatives will be able to occupy the empty orbitals to form coordinate covalent bonds]. Hexaaza-18-crown-6 which has more nitrogen (N) heteroatoms bound to the crown ether ring can form more stable complex compounds with iron metal (Fe), so that hexaaza-18-crown-6 has better inhibition ability compared to other inhibitors.

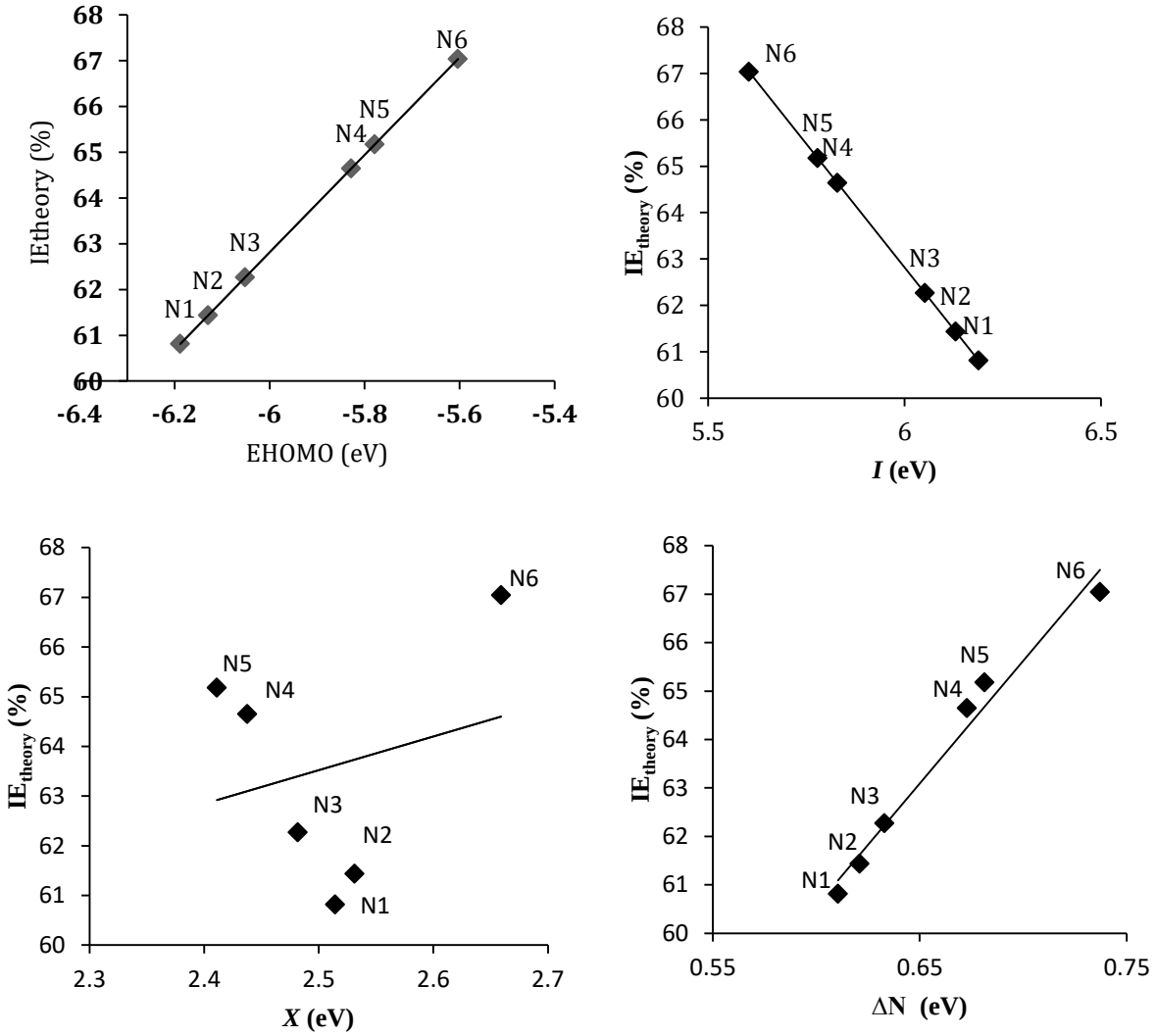

Figure 3. Relationship between HOMO energy and inhibition efficiency

HOMO energy is the molecular orbital with the highest energy level that will be occupied by electrons. LUMO energy is the molecular orbital with the lowest energy level that is not occupied by electrons. HOMO energy is the property of molecules to donate electrons. The higher the HOMO energy, the stronger an organic compound's adhesion to a metal surface, resulting in higher efficienc. Conversely, the lower the LUMO energy, the more readily the molecule accepts electrons. Inhibitor molecules function to donate their lone pairs of electrons to the iron metal. Therefore, more reactive inhibitors are those with higher HOMO energies and lower LUMO energies [22].

Based on the data in Table 2, the EHOMO values of the aza-18-crown-6

derivative compounds can be sorted from the highest to the lowest, namely hexaaza-18-crown-6 (N6) > pentaaza-18-crown-6 (N5) > tetraaza-18-crown-6 (N4) > triaza-18-crown-6 (N3) > diaza-18-crown-6 (N2) > monoaza-18-crown-6 (N1). The effect of EHOMO on corrosion inhibition efficiency can be clarified by the correlation in Figure 3.

Figure 3 shows the relationship between HOMO energy and inhibition efficiency, indicating that a higher HOMO energy value increases corrosion inhibition efficiency. This EHOMO value is directly proportional to the corrosion inhibition efficiency of aza-18-crown-6 derivatives. Corrosion inhibition efficiency increases for the organic inhibitor hexaaza-18-crown-6 (N6), which has the highest HOMO energy value of -5.60364 eV. The lowest HOMO energy is for the organic inhibitor monoaza-18-crown-6 (N1), which has a HOMO energy value of -6.18814 eV, thus decreasing corrosion inhibition efficiency.

A high EHOMO energy value indicates that the organic inhibitor compound is highly susceptible to excitation to the empty d orbital on iron. This occurs because organic inhibitors with a high EHOMO have lone electron pairs, such as nitrogen atoms (N), which have a high electron density. Therefore, the electrons from these compounds can interact with iron, forming bonds that coat the iron surface, increasing its corrosion inhibition efficiency Therefore, the inhibitor hexaaza-18-crown-6 (N6) has a higher inhibition efficiency compared to other inhibitors because it is more easily excited.

Ionization potential is the energy required to remove one outermost electron from an atom. Ionization potential is used to measure the reactivity of an atom or molecule. A high ionization potential value indicates high reactivity, while a low ionization potential value indicates low reactivity. Based on Table 2, the order of ionization potential values from smallest to largest is hexaaza-18-crown-6 (N6) < pentaaza-18-crown-6 (N5) < tetraaza-18-crown-6 (N4) < triaza-18-crown-6 (N3) < diaza-18-crown-6 (N2) < monoaza-18-crown-6 (N1). The effect of ionization potential on corrosion inhibition efficiency can be clarified by the correlation graph in Figure 3.

Figure 3 shows that ionization potential has a significant effect on corrosion inhibition efficiency. The ionization potential is inversely proportional to the corrosion inhibition efficiency. The lower the ionization potential, the higher the inhibition efficiency, and conversely, the higher the ionization potential, the lower the inhibition efficiency. Ionization potential is defined as the amount of energy required to remove one outermost electron from an atom. This is certainly related to the attraction between the nucleus and the electron. The higher the ionization potential, the greater the attraction of the electron to the atomic nucleus, and the greater the energy required for the electron to escape from its orbit. Conversely, the lower the ionization potential, the smaller the attraction of the electron to the atomic nucleus, and the lower the energy required for the electron to escape or exit its orbit, making the molecule more reactive

Table 2 shows that the ionization potential of the hexaaza-18-crown-6 (N6) inhibitor is lower, at 5.60365 eV, while the ionization potential of the monoaza-18-crown-6 (N1) inhibitor is higher, at 6.18814 eV. Based on these data, it can be predicted that the hexaaza-18-crown-6 (N6) inhibitor has a higher inhibition efficiency, allowing electrons to be easily released to bind to iron compared to the monoaza-18-crown-6 (N1) inhibitor. Electronegativity is the ability of an atom in a molecule to attract electrons into its atomic structure. Electronegativity is the affinity of an atom to attract electrons in a bond. A low electronegativity value makes it easier for a molecule to reach electron equilibrium, making it less reactive. A high electronegativity value indicates a more difficult time for a molecule to reach equilibrium, making it more reactive [23].

The electronegativity ranking, from highest to lowest, is hexaaza-18-crown-6 (N6) > diaza-18-crown-6 > monoaza-18-crown-6 (N1) > triaza-18-crown-6 (N3) > tetraaza-18-crown-6 (N4) > pentaaza-18-crown-6 (N5). The effect of electronegativity on corrosion inhibition efficiency can be clarified by the correlation in Figure 3. Figure 3 shows that the relationship between electronegativity and corrosion inhibition efficiency is not well correlated. Data in Table 4.2 shows that corrosion inhibition efficiency increases with the hexaaza-18-crown-6 (N6) inhibitor, which has a higher electronegativity value of 2.65909 eV. This indicates that hexaaza-18-crown-6 (N6) has a higher electron-attracting capacity than other inhibitor compounds, and therefore, hexaaza-18-crown-6 (N6) is a better inhibitor than other

inhibitors. Meanwhile, several researchers have stated that low electronegativity values can cause molecules to more easily reach electron equilibrium, making them more reactive, and vice versa. A literature survey found several deviations in the correlation between electronegativity and corrosion inhibition efficiency, making electronegativity an unsuitable parameter for determining corrosion inhibition efficiency.

Electron transfer is the ability to donate electrons, thus determining the number of electrons transferred from an organic inhibitor as a donor molecule to an iron metal as an acceptor atom. The electron transfer value significantly influences corrosion inhibition efficiency. The order of electron transfer values from highest to lowest is hexaaza-18-crown-6 (N6) > pentaaza-18-crown-6 (N5) > tetraaza-18-crown-6 (N4) > triaza-18-crown-6 (N3) > diaza-18-crown-6 (N2) > monoaza-18-crown-6 (N1).

Figure 3 shows that electron transfer significantly influences the corrosion inhibition efficiency of aza-18-crown-6 derivatives. This electron transfer value is directly proportional to the corrosion inhibition efficiency. The higher the electron transfer value, the higher the corrosion inhibition efficiency. Based on the data in Table 4.2, the electron transfer value of the hexaaza-18-crown-6 (N6) inhibitor is higher at 0.73710 eV, thus having a higher corrosion inhibition efficiency. Meanwhile, the electron transfer value of the monoaza-18-crown-6 (N1) inhibitor is lower at 0.61049 eV, thus having a lower corrosion inhibition efficiency.

Electron transfer describes the ease with which a molecule can donate electrons, rather than measuring the number of electrons transferred. A molecule's corrosion inhibition ability increases with the ease with which it donates electrons to the metal surface, thus inhibiting the corrosion process. Therefore, the hexaaza-18-crown-6 (N6) inhibitor has a higher inhibition efficiency compared to other inhibitors because it is more readily able to donate its electrons.

Electrostatic Surface Potential (ESP) Analysis

Electrostatic Surface Potential (ESP) is the probability of finding an electron at Cartesian coordinates (x, y, and z) within a molecule. The electrostatic surface potential is often associated with electron density. Electron density is the region where electrons can be found. Electron density can explain molecular properties, reactivity, and stability. High electron density indicates regions with a high probability of electron occupancy, while the converse is true for regions with low electron density, which also have a low probability of electron occupancy. ESP provides a visual method for understanding the relative polarity of a molecule. Red indicates regions with high electronegativity, such as oxygen (O) and nitrogen (N) atoms. Yellow represents atoms with moderate electronegativity. Blue indicates positive regions for organic inhibitors. The ESP visualization results for the aza-18-crown-6 derivative compound can be seen in Figure 4.

Figure 4 shows that all organic inhibitors (monoaza-18-crown-6, diaza-18-crown-6, triaza-18-crown-6, tetraaza-18-crown-6, pentaaza-18-crown-6, hexaaza-18-crown-6) have oxygen and nitrogen atoms with high electron density in the red region, indicating a uniform distribution of electrons in the heteroatom-containing crown ether ring. Based on the ESP visualization results, hexaaza-18-crown-6 has a higher electron density than the other inhibitor compounds. This is evident from the abundance of red in the crown ether ring, indicating an electron-rich region or region with the highest electron density. This region with the highest electron density is the region with the highest probability of electrons being found, making it the most favorable region for the iron (Fe) metal surface during the adsorption process.

Monte Carlo Simulation

Monte Carlo simulations were conducted to understand the interaction mechanism of organic inhibitors and iron metal surfaces. Previous Monte Carlo studies have shown a very strong molecular attraction between organic inhibitors and metal surfaces. The Monte Carlo simulation process attempts to find the lowest energy for all systems. The Monte Carlo simulation process was performed on organic inhibitors derived from aza-18-crown-6 compounds, such as (monoaza-18-crown-6, diaza-18-crown-6, triaza-18-crown-6, tetraaza-18-crown-6, pentaaza-18-crown-6, hexaaza-18-crown-6), using 100 water molecules and an iron metal surface with an Fe (110) plane. The Monte Carlo visualization results can be seen in Figure 5.

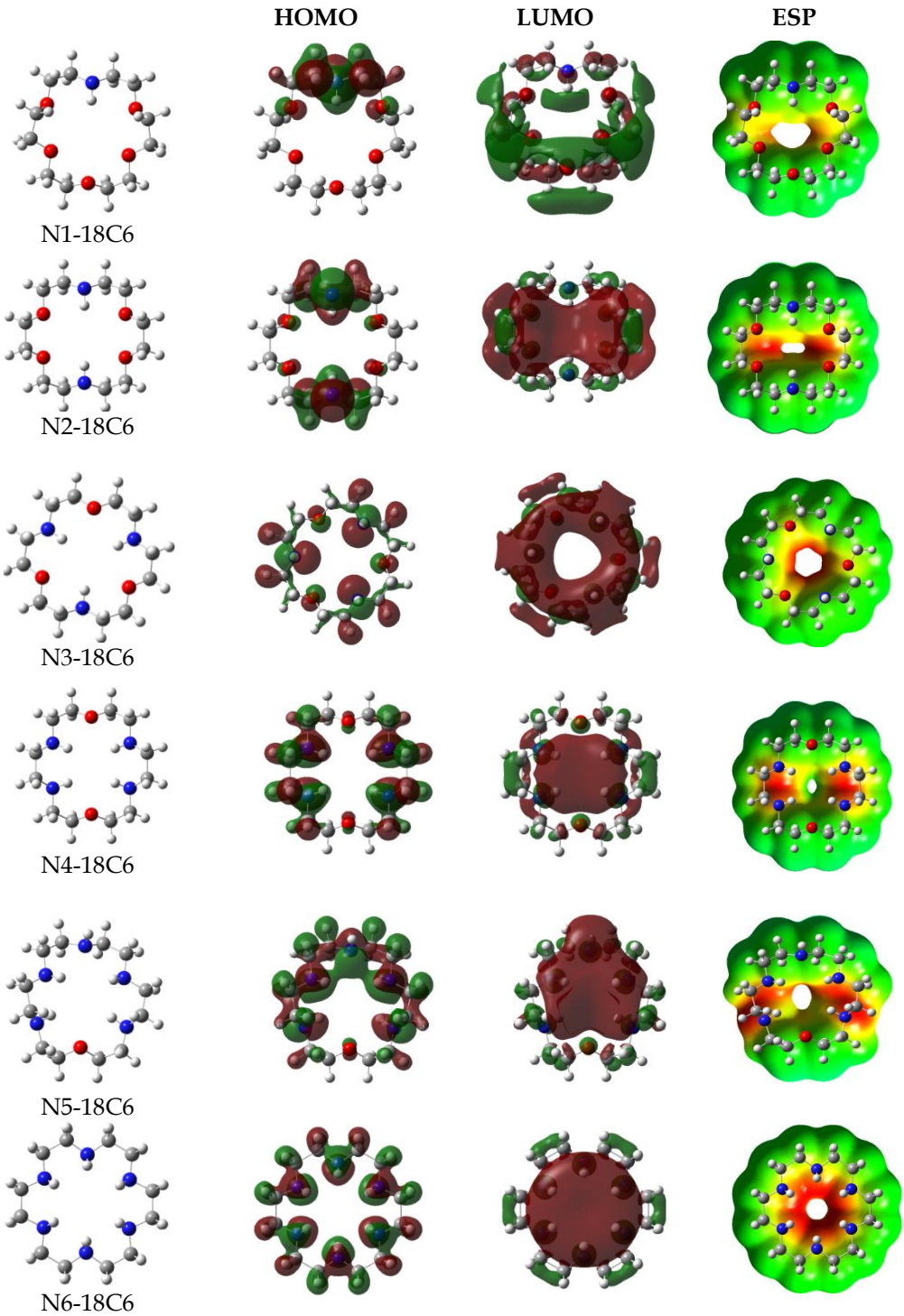

Figure 4. HOMO-LUMO and ESP energy visualization of aza-18-crown-6 derivatives

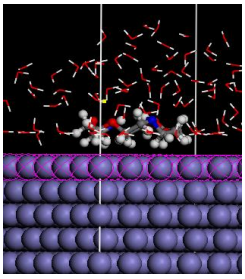
Fe(110)/N118C6/100H_2O

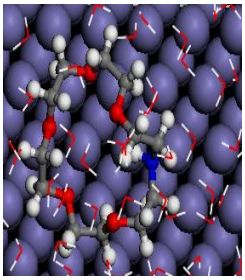
Fe(110)/N118C6/100H_2O

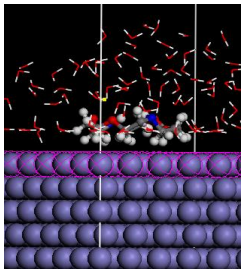
Fe(110)/N218C6/100H_2O

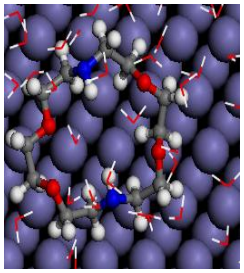
Fe(110)/ N218C6/100H_2O

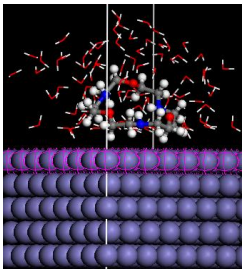
Fe(110)/N318C6/100H_2O

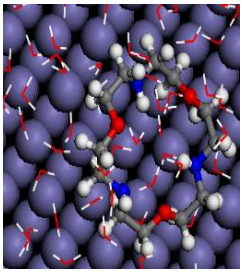
Fe(110)/N318C6/100H_2O

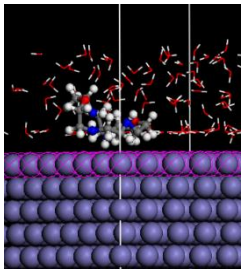
Fe(110)/N418C6/100H_2O

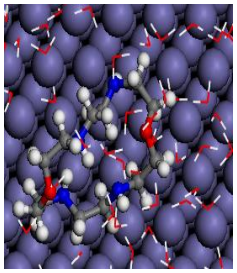
Fe(110)/N418C6/100H_2O

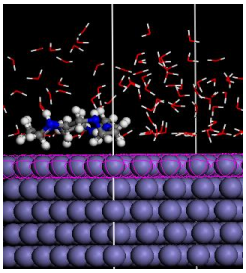
Fe(110)/N518C6/100H_2O

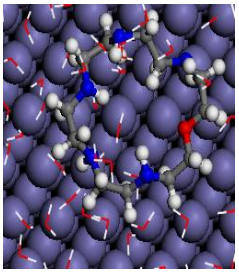
Fe(110)/N518C6/100H_2O

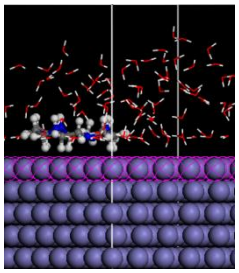
Fe(110)/ N618C6/100H_2O

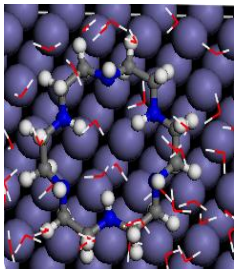
Fe(110)/N618C6/100H_2O

Figure 5. Visualization Monte Carlo

Table 4 Adsorption energy of Fe(110)/Inhibitor/100H2O

Systems	Adsorption Energy (inhibitor) kJ.mol^{-1}	Adsorption Energy (H_2O) kJ.mol^{-1}
Fe(110)/N118C6/100H_2O	-169.4304	-17.7823
Fe(110)/N218C6/100H_2O	-171.8455	-17.3577
Fe(110)/N318C6/100H_2O	-175.3810	-16.7508
Fe(110)/N418C6/100H_2O	-181.3174	-16.4385
Fe(110)/N518C6/100H_2O	-187.4716	-17.2814
Fe(110)/N618C6/100H_2O	-196.6356	-17.2892

Figure 5 shows that the results of Monte Carlo simulations with the most stable adsorption conformation of each organic inhibitor of the aza-18-crown-6 derivative compound on the surface of Fe (110) and 100 water molecules. The distance between atoms in the organic inhibitor and the metal surface can help to understand the nature of the adsorption process. Based on the visualization results, the structure of the hexaaza-18-crown-6 (N6) compound is bound very strongly to the surface of iron metal (Fe) compared to other inhibitors. This is due to the presence of more nitrogen (N) heteroatoms in the hexaaza-18-crown-6 compound which can increase the electron density in its molecular structure, thus facilitating a greater adsorption process compared to other inhibitor compounds. The large adsorption process by the hexaaza-18-crown-6 ligand on the iron metal surface

indicates the greater ability of hexaaza-18-crown-6 in protecting iron metal (Fe) from corrosive substances in solution than other inhibitors. Based on Table 4.3, the adsorption sequence of organic inhibitor compounds on the surface of iron metal is hexaaza-18-crown-6 (N6) > pentaaza-18-crown-6 (N5) > tetraaza-18-crown-6 (N4) > triaza-18-crown-6 (N3) > diaza-18-crown-6 (N2) > monoaza-18-crown-6 (N1).

This sequence is the same or in accordance with the results obtained from DFT/B3LYP 6-311G (d,p) quantum calculations in the solution phase. Organic inhibitors (monaza-18-crown-6, diaza-18-crown-6, triaza-18-crown-6, tetraaza-18-crown-6, pentaaza-18-crown-6, hexaaza-18-crown-6) have lone electron pairs such as nitrogen atoms (N) in the cavity of the crown ether ring, so that it can allow to donate electrons to empty d orbitals on the Fe (110) surface and can form stable coordination bonds. Higher negative adsorption energy values indicate more stable and stronger interactions between organic inhibitors and iron metal. Based on Table 4.3, it shows that the adsorption energy value of the organic inhibitor hexaaza-18-crown-6 (N6) is obtained at -196.6356 kcal/mol higher to the metal surface than other inhibitors. So that the organic inhibitor structure of hexaaza-18-crown-6 (N6) can cover and form a protective layer of iron metal that is larger than other inhibitors from corrosive substances in solution.

Conclusion

The DFT method at the B3LYP level of theory with the 6-31G(d) basis set was the best method selected based on validation of the method comparing the geometric structure and bond lengths of experimental studies with theoretical results. The addition of nitrogen heteroatoms can affect the corrosion inhibition efficiency of aza-18-crown-6 derivatives. This is because nitrogen heteroatoms cause a greater distribution of electrons in the crown ether ring, resulting in more electrons being donated to iron. Quantum parameters indicate that inhibition efficiency increases with the hexaaza-18-crown-6 (N6) inhibitor compound, reaching 67.037%.

Acknowledgments

The authors gratefully acknowledge Universitas Mataram for providing access to computational laboratory facilities and technical support essential for conducting the simulation work presented in this study.

Author Contributions

Conceptualization, S.H. and E.J.; methodology, N.A.; software, N.A.; validation, SH., E.J. and A.A.; formal analysis, N.A.; investigation, N.A.; resources, N.A.; data curation, N.A.; writing—original draft preparation, N.A.; writing—review and editing, S.H.; visualization, N.A.; supervision, N.A.; funding acquisition, S.H. All authors have read and agreed to the published version of the manuscript

Conflicts of Interest

The authors declare no conflict of interest

References

1. Quadri, T. W., Akpan, E. D., Olasunkanmi, L. O., Fayemi, O. E., & Ebenso, E. E. (2022). Fundamentals of corrosion chemistry. In *Environmentally sustainable corrosion inhibitors* (pp. 25-45). Elsevier.
2. Zehra, S., Mobin, M., Parveen, M., & Ahmad, R. (2025). Corrosion Fundamentals: Understanding the Science Behind the Damage. *Industrial Corrosion: Fundamentals, Failure, Analysis and Prevention*, 1-16.
3. Sheetal, Batra, R., Singh, A. K., Singh, M., Thakur, S., Pani, B., & Kaya, S. (2023). Advancement of corrosion inhibitor system through N-heterocyclic compounds: a review. *Corrosion Engineering, Science and Technology*, *58*(1), 73-101.
4. Verma, D. K., Dewangan, Y., Dewangan, A. K., & Asatkar, A. (2021). Heteroatom-based compounds as sustainable corrosion inhibitors: an overview. *Journal of Bio-and Tribo-Corrosion*, *7*(1), 15.
5. Abdallah, M., Fouda, A. S., & El, A. S. (2008). Corrosion inhibiting properties of some crown ethers on corrosion of stainless steel (types 304 and 316) in hydrochloric acid. *Zaštita materijala*, *49*(3), 9-22.
6. Al-Mazaideh, G. (2019). Corrosion and electrochemical studies on the stability of new thiacrown ethers derived from quinoline. *Jordan Journal of Chemistry (JJC)*, *14*(3), 89-96.
7. Hadisaputra, S., Purwoko, A. A., Rahmawati, Hamdiani, S., Prananto, Y. P., & Nuryono. (2019, June). Theoretical study on the corrosion inhibition performance of dibenzo-18-crown-6 and its derivatives. In *IOP Conference Series: Materials Science*

and Engineering (Vol. 546, No. 3, p. 032011). IOP Publishing.
8. Hadisaputra, S., Hamdiani, S., Kurniawan, M. A., & Nuryono, N. (2017). Influence of macrocyclic ring size on the corrosion inhibition efficiency of dibenzo crown ether: a density functional study. *Indonesian Journal of Chemistry*, *17*(3), 431-438.
9. Hasanov, R., Bilge, S., Bilgiç, S., Gece, G., & Kılıç, Z. (2010). Experimental and theoretical calculations on corrosion inhibition of steel in 1 M H2SO4 by crown type polyethers. *Corrosion Science*, *52*(3), 984-990.
10. Fouda, A. S., Abdallah, M., Al-Ashrey, S. M., & Abdel-Fattah, A. A. (2010). Some crown ethers as inhibitors for corrosion of stainless steel type 430 in aqueous solutions. *Desalination*, *250*(2), 538-543.
11. Paul, P. K., Yadav, M., & Obot, I. B. (2021). Potential of dibenzo-18-crown-6-ether derivatives as a corrosion inhibitor on mild steel in HCl medium: electrochemical and computational approaches. *New Journal of Chemistry*, *45*(15), 6826-6842.
12. Zhan, C. G., Nichols, J. A., & Dixon, D. A. (2003). Ionization potential, electron affinity, electronegativity, hardness, and electron excitation energy: molecular properties from density functional theory orbital energies. *The Journal of Physical Chemistry A*, *107*(20), 4184-4195.
13. Pal, R., & Chattaraj, P. K. (2023). Electrophilicity index revisited. *Journal of Computational Chemistry*, *44*(3), 278-297.
14. Sabin, J. R., Trickey, S. B., Apell, S. P., & Oddershede, J. (2000). Molecular shape, capacitance, and chemical hardness. *International Journal of Quantum Chemistry*, *77*(1), 358-366.
15. El Azzouzi, M., Aouniti, A., Tighadouin, S., Elmsellem, H., Radi, S., Hammouti, B., ... & Zarrouk, A. (2016). Some hydrazine derivatives as corrosion inhibitors for mild steel in 1.0 M HCl: weight loss, electrochemichal, SEM and theoretical studies. *Journal of Molecular Liquids*, *221*, 633-641.
16. Obayes, H. R., Alwan, G. H., Alobaidy, A. H. M., Al-Amiery, A. A., Kadhum, A. A. H., & Mohamad, A. B. (2014). Quantum chemical assessment of benzimidazole derivatives as corrosion inhibitors. *Chemistry Central Journal*, *8*(1), 21.
17. Verma, C., Obot, I. B., Bahadur, I., Sherif, E. S. M., & Ebenso, E. E. (2018). Choline based ionic liquids as sustainable corrosion inhibitors on mild steel surface in acidic medium: Gravimetric, electrochemical, surface morphology, DFT and Monte Carlo simulation studies. *Applied Surface Science*, *457*, 134-149.
18. Hadisaputra, S., Purwoko, A. A., Hakim, A., Prasetyo, N., & Hamdiani, S. (2022). Corrosion inhibition properties of phenyl phthalimide derivatives against carbon steel in the acidic medium: DFT, MP2, and Monte Carlo simulation studies. *ACS omega*, *7*(37), 33054-33066.
19. Dunitz, J. D., Dobler, M., Seiler, P., & Phizackerley, R. P. (1974). Crystal Structure Analyses of 1,4,7,10,13,16-Hexaoxacyclooctadeeane and its Complexes with Alkali Thiocyanates. *Acta Cryst, B30*, 2733-2737
20. Verma, C., Verma, D. K., Ebenso, E. E., & Quraishi, M. A. (2018). Sulfur and phosphorus heteroatom-containing compounds as corrosion inhibitors: An overview. *Heteroatom Chemistry*, *29*(4), e21437.
21. Islam, N., & Ghosh, D. C. (2014). The Time Evolution of the Hard and Soft Acids and Bases Theory. *Theoretical and Computational Research in the 21st Century*, *1*.
22. Abeng, F. E., Thakur, A., Anadebe, V. C., & Ebenso, E. E. (2025). A comparative density functional theory (DFT) and molecular dynamics study on Natamycin and Cefmetazole as effective corrosion inhibitor for mild steel: Electronic properties and adsorption behavior. *Computational and Theoretical Chemistry*, *1248*, 115200.
23. Ekeocha, C. I., Uzochukwu, I. N., Onyeachu, I. B., Etim, I. I. N., & Oguzie, E. E. (2025). Theoretical study of novel antipyrine derivatives as promising corrosion inhibitors for mild steel in an acidic environment. *Structural Chemistry*, *36*(1), 363-379.
24. Othman, K. A., Hamad, W. M., & Omer, R. A. (2025). Theoretical and experimental exploration of organic molecules adsorption on iron surfaces for corrosion inhibition: a review. *Corrosion Reviews*, *43*(3), 335-359.
25. Yan, Q., Hou, L., Sun, J., Li, D., Song, J., Liu, X., ... & Wei, Y. (2025). Regulating the localized corrosion of grain boundary and galvanic corrosion by adding the electronegative element in magnesium alloy. *Corrosion Science*, *244*, 112667.